Compact, 1.5 mJ, 450 MHz, $CdSiP_2$ picosecond optical parametric oscillator near 6.3 μm

S. Chaitanya Kumar,[1,*] A. Agnesi,[2] P. Dallocchio,[2] F. Pirzio,[2] G. Reali,[2] K. T. Zawilski,[3] P. G. Schunemann,[3] and M. Ebrahim-Zadeh[1,4]

[1]*ICFO-Institut de Ciencies Fotoniques, Mediterranean Technology Park, 08860 Castelldefels, Barcelona, Spain*

[2]*Laser Source Laboratory–University of Pavia, Department of Electronics, via Ferrata 1–27100 Pavia, Italy*

[3]*BAE Systems, Incorporated, MER15-1813, P.O. Box 868, Nashua, New Hampshire 03061-0868, USA*

[4]*Institucio Catalana de Recerca i Estudis Avancats (ICREA), Passeig Lluis Companys 23, Barcelona 08010, Spain*

**Corresponding author: chaitanya.suddapalli@icfo.es*

Received June 6, 2011; accepted July 15, 2011;
posted July 21, 2011 (Doc. ID 148770); published August 15, 2011

We report a compact, efficient, high-energy, and high-repetition-rate mid-IR picosecond optical parametric oscillator (OPO) based on the new nonlinear material $CdSiP_2$ (CSP). The OPO is synchronously pumped by a master oscillator power amplifier system at 1064.1 nm, providing 1 μs long macropulses constituting 8.6 ps micropulses at 450 MHz, and it can be tuned over 486 nm across 6091–6577 nm, covering the technologically important wavelength range for surgical applications. Using a compact (~30 cm) cavity and improved, high-quality nonlinear crystal, idler macropulse energy as high as 1.5 mJ has been obtained at 6275 nm at a photon conversion efficiency of 29.5%, with >1.2 mJ over more than 68% of the tuning range, for an input macropulse energy of 30 mJ. Both the signal and idler beams are recorded to have good beam quality with a Gaussian spatial profile, and the extracted signal pulses are measured to have durations of 10.6 ps. Further, from the experimentally measured transmission data at 1064 nm, we have estimated the two-photon absorption coefficient of CSP to be $\beta = 2.4$ cm/GW, with a corresponding energy bandgap, $E_g = 2.08$ eV.

OCIS codes: 190.4400, 190.4970, 190.7110, 170.6935.

The mid-IR window of the optical spectrum has a wealth of information pertaining to many molecules of importance involved in a variety of applications, from surgery [1] to explosive detection [2]. In particular, mid-IR radiation in the 5900–6600 nm wavelength range, constituting the absorption bands of amide I (6000), water (6100), and amide II (6450 nm) are of interest for human surgery because of the simultaneous absorption by both proteins and water. Past research has shown that the choice of these wavelengths minimizes the collateral damage while maintaining an effective ablation rate of the tissue, enabling minimally invasive human surgery [1]. In the absence of conventional lasers at these wavelengths, the free electron laser has been shown to be the only source capable of delivering sufficient energy for such applications [3]. But its high complexity, large size, and high cost preclude its use in practical applications.

Optical parametric oscillators (OPOs) are recognized as powerful and viable solid-state sources of coherent radiation, providing access to mid-IR spectral region with wide tunability. However, mid-IR OPOs, pumped at 1 μm have relied mainly on oxide-based nonlinear materials such as $LiNbO_3$, practically limiting the spectral coverage of these devices to ~4 μm, imposed by the onset of absorption [4]. Alternatively, OPOs based on chalcopyrite crystals such as AgGaSe and the most developed $ZnGeP_2$ can generate mid-IR radiation up to ~10 μm, but they must be pumped above 1 μm to avoid two-photon and residual absorption. As a result, they are often pumped in tandem, typically by another OPO, resulting in complex architectures [4]. Hence, it is imperative to explore viable alternative materials for generation of mid-IR radiation beyond 4 μm pumped by Nd-based solid-state lasers at 1064 nm. The quest for such a nonlinear material recently led to the development of $CdSiP_2$ (CSP) [5]. Its large bandgap, high optical quality, improved thermal and optical properties with high effective nonlinear coefficient (d_{eff}~84.5 pm/V), and noncritical phase-matching (NCPM) make it an attractive nonlinear material candidate for generating mid-IR wavelengths in the 6–6.5 μm range.

Earlier reports on mid-IR OPOs based on CSP pumped at 1064 nm include a low-repetition-rate (10 Hz) nanosecond oscillator with idler energies up to 0.47 mJ at 6.2 μm [6] and a 0.24 mJ, 1 kHz, subnanosecond OPO with idler tuning around 6.1 μm [7]. Also, mid-IR picosecond pulses near 6.4 μm with an output energy of 0.56 mJ were generated by synchronous pumping an OPO with a nonlinear mirror mode-locked Nd:YAG laser in noncollinear geometry [8]. Recently, single-pass parametric generation in CSP was also reported, pumped at 1064 nm, providing picosecond pulses with energy of 1.54 μJ at 6.2 μm at a repetition rate of 100 kHz [9].

Here, we report a compact, high-repetition-rate OPO based on CSP, synchronously pumped by a master oscillator power amplifier (MOPA) system at 1064.1 nm, generating an idler energy as high as 1.5 mJ at 6246 nm with a photon conversion efficiency of 29.5%. The OPO is tunable over 486 nm, with more than 1.2 mJ over >68% of the tuning range in good beam quality. To our knowledge, this is the first high-repetition-rate picosecond CSP OPO, synchronously pumped at 1064 nm in collinear geometry.

The schematic of the experimental setup is shown in Fig. 1. The high-energy MOPA pump laser system is seeded by a 450 MHz passively mode-locked oscillator providing 5.4 ps micropulses. An acousto-optic modulator selects a train of micropulses with 1 μs duration (macropulse) at a repetition rate of 20 Hz, and the successive amplifier stages increase the macropulse energy up to 50 mJ, corresponding to an average power of 1 W. This

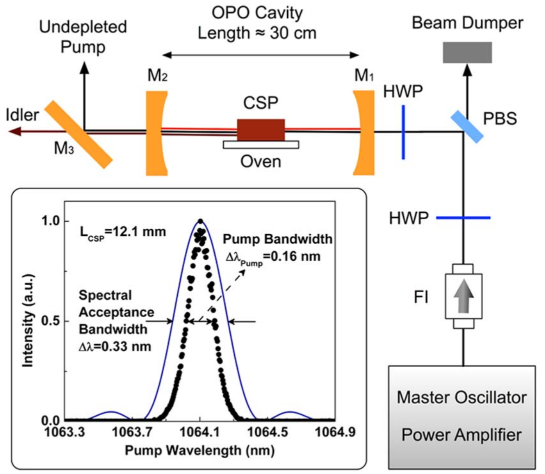

Fig. 1. (Color online) Experimental setup of synchronously pumped, high-energy picosecond OPO: FI, Faraday isolator; HWP, half-wave plate; PBS, polarization beam splitter; M, mirrors. Inset, pump laser spectrum relative to parametric gain bandwidth for a 12.1 mm long CSP crystal.

represents an average single micropulse energy of 0.1 mJ with a measured pulse width of 8.6 ps.

The pump laser operates at a central wavelength of 1064.1 nm and has an FWHM spectral bandwidth of 0.16 nm. This is shown in the inset of Fig. 1, relative to the parametric gain bandwidth of 0.33 nm for 12.1 mm long CSP crystal, estimated using the relevant Sellmeier equations [5]. The output beam from the pump laser has a diameter of 2 mm and a quality factor of $M^2 \sim 1.1$. The CSP crystal is a 12.1 mm long, 4 mm wide (along the c axis), 5 mm thick sample grown from stoichiometric melt by the horizontal gradient freeze technique [5]. It is cut at $\theta = 90°$, $\phi = 45°$ for Type I ($e \rightarrow oo$) interaction under NCPM and housed in an oven with temperature stability of ±0.1 °C. Both crystal faces are antireflection coated with a single-layer sapphire coating, providing high transmission ($T > 98.7\%$) for the pump and signal over 1064–1300 nm and $T > 76\%$ for the idler over 6000–6500 nm. The residual loss at 1064.1 nm is estimated from the measured transmission of the crystal. As depicted in Fig. 2, we observed a drop in the transmission of the CSP crystal with increasing pump intensity, showing a nonlinear behavior. Using a simple two-photon absorption model, we fitted the measured data for linear (α) and two-photon (β) absorption coefficients, resulting in a value of $\alpha = 0.075\ \mathrm{cm}^{-1}$, $\beta = 2.4\ \mathrm{cm/GW}$ for *extraordinary* (e) and $\alpha = 0.15\ \mathrm{cm}^{-1}$, $\beta = 2.6\ \mathrm{cm/GW}$ for *ordinary* (o) polarizations. These values indicate the improved quality of this crystal as compared to the earlier samples [6–9]. Further, using these data, we have estimated the energy bandgap (E_g) resulting in the values of 2.08 eV (e) and 2.06 eV (o), confirming the large bandgap of CSP [10]. The OPO is configured as a singly resonant oscillator in a compact linear standing wave cavity comprising two curved mirrors, M_1 and M_2, with radius of curvature $r = 3\,m$ (ZnSe substrate). Both mirrors are highly reflecting ($R > 99\%$) for a signal over 1200–1400 nm, and highly transmitting at 1064 nm ($T > 97\%$) and for the idler over 5500–7500 nm ($T > 98\%$). The pump beam has a radius of $w_0 \sim 1.5$ mm after the input mirror (M_1) to avoid any damage, while using the

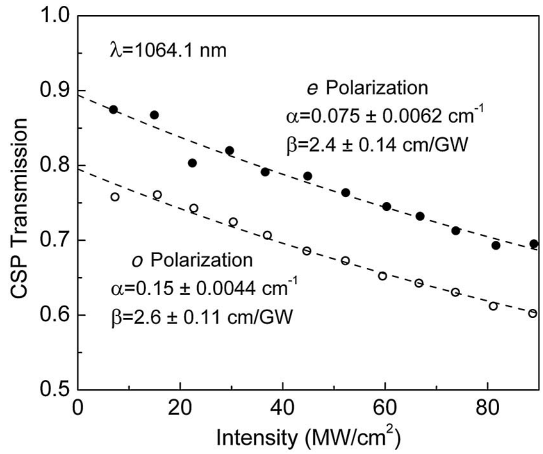

Fig. 2. CSP transmission as a function of pump intensity for o polarization and e polarization at 1064.1 nm.

maximum aperture of the crystal. A dichroic mirror, M_3, highly reflecting ($R > 99\%$) at 1064 nm and highly transmitting ($T > 95\%$) for the idler, separates the generated idler from the undepleted pump. In the measurements of energy and efficiency, all the data were corrected for transmission and reflection coating losses. The total round-trip optical length of the cavity, including the CSP crystal, is 666 mm, corresponding to a 450 MHz repetition rate, ensuring the synchronization with the pump laser.

Figure 3 shows the extracted idler energy as well as the transmission of the CSP crystal across the tuning range, at a constant pump energy of 30 mJ. Using a 500 μm fused silica etalon, we extracted part of the intracavity signal to monitor the wavelength. The signal wavelength was recorded by using a low-resolution (~10 nm) InGaAs spectrometer (Ocean Optics, NIR Quest), and it was further confirmed by single-pass second harmonic generation into the red in a 5 mm Type I ($oo \rightarrow e$) BBO crystal. The idler wavelength was inferred from the second harmonic of the signal, which was measured using a high-resolution (~1 nm) CCD array spectrometer (Ocean optics, USB 4000).

By changing the CSP crystal temperature from 30 °C to 180 °C, we could tune the idler from 6091 to 6577 nm, corresponding to a total tuning range of 486 nm. The generated idler energy varies from 1.3 mJ at 6091 nm to 1 mJ at 6577 nm, reaching a maximum of 1.5 mJ at 6275 nm, with

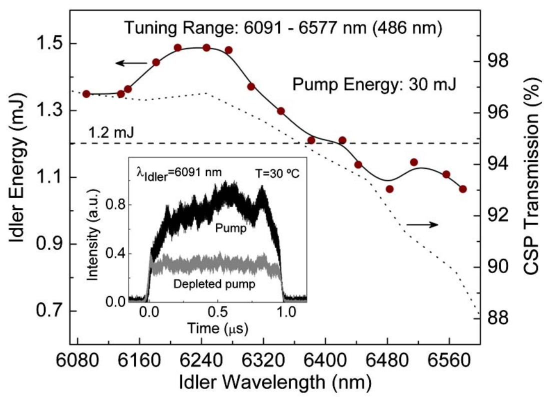

Fig. 3. (Color online) Idler energy and CSP transmission across the tuning range. Inset, macropulse envelope of the input pump and the depleted pump.

>1.2 mJ over >68% of the tuning range. This represents a maximum idler energy conversion efficiency of 5% and a photon conversion efficiency of 29.5%. The drop in the idler energy toward the longer wavelengths is attributed to the water absorption peak near 6.4 μm and residual multiphonon absorption in the CSP crystal, resulting in reduced transmission, as is evident in Fig. 3. The corresponding pump depletion is recorded to be >42% over more than 64% of the tuning range with a maximum pump depletion of 51% at 6483 nm. Also shown, in the inset of Fig. 3, is the macropulse envelope of the input and the depleted pump, measured using a fast photodiode, at 30 °C (idler wavelength of 6091 nm), clearly showing >50% depletion.

The variation of the idler energy and pump depletion as a function of the pump energy obtained at a temperature of 30 °C (idler wavelength of 6091 nm) is shown in Fig. 4. As is evident from the plot, 1.35 mJ of the idler is obtained for a pump energy of 30 mJ at a slope efficiency of $\eta = 4.6\%$, implying a peak idler energy efficiency of 4.5%, representing a photon conversion efficiency of 25.7%. The threshold pump energy is measured to be 0.7 mJ, corresponding to a single micropulse energy of 1.5 μJ, and strong pump depletion reaching >50% is achieved above the input pump energy of 5 mJ. The peak efficiency in this experiment was limited by the low optical damage threshold of the single-layer sapphire coating on the CSP crystal, observed beyond 30 mJ of pump energy. Increasing the pump energy to 31.5 mJ, representing a peak intensity of $100\ \mathrm{MW/cm^2}$, resulted in surface damage on the input face of the crystal, while no damage was observed on the exit face, indicating that the damage is due to the pump beam. Although the damage did not prevent OPO operation, a substantial drop of 37% in the idler energy was noticed. We also characterized the OPO near 6400 nm, a technologically important wavelength for surgical applications [1], as is shown in the inset of Fig. 4. At 130 °C, corresponding to an idler wavelength of 6422 nm, idler energy up to 1.1 mJ is generated for pump energy of 30 mJ at a slope efficiency of $\eta = 3.8\%$, with an increased threshold pump energy of 1.6 mJ due to water absorption and reduced crystal transmission.

Figure 5(a) shows the measured autocorrelation profile at a signal wavelength of 1289 nm, where the amount of

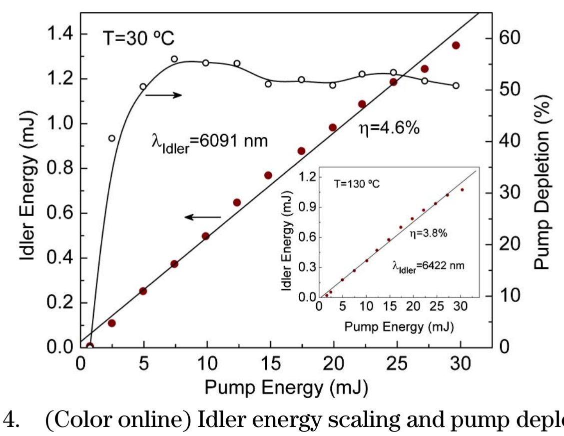

Fig. 4. (Color online) Idler energy scaling and pump depletion as a function of input pump energy at $\lambda_{\mathrm{Idler}} = 6091$ nm. Inset, idler energy scaling at 6422 nm.

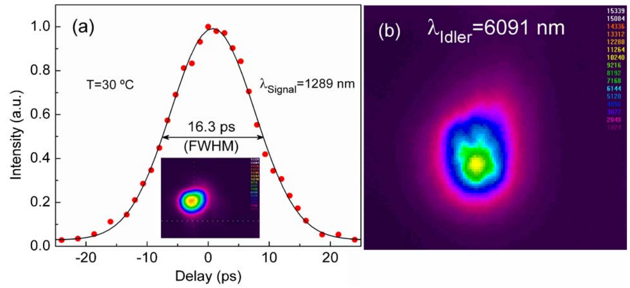

Fig. 5. (Color online) (a) Typical autocorrelation of the OPO signal pulse at 1289 nm, with a duration of 10.6 ps (×1.54, assuming a sech^2 pulse shape). Inset, signal beam profile at 1289 nm. (b) Spatial beam profile of the idler pulse at 6091 nm.

signal energy extracted from the cavity was >1.3 mJ for an incident pump energy of 30 mJ. The FWHM of the trace is 16.3 ps, resulting in the signal pulse duration of 10.6 ps, assuming a sech^2 pulse shape. This value of the pulse duration was confirmed by repeating the measurement several times, and a similar pulse duration is expected across the tuning range. Also shown, in the inset of Fig. 5(a), is the signal beam profile at 1289 nm, measured using a pyroelectric camera (Spiricon, Pyrocam III). The corresponding idler beam profile at 6091 nm, recorded at the full output energy, is shown in Fig. 5(b). Both signal and idler exhibit good beam quality with Gaussian profiles, which is important for surgical applications.

In conclusion, we demonstrated a compact, 1.5 mJ, 450 MHz, CSP OPO tunable from 6091 to 6577 nm for surgical applications in the mid-IR.

This research was supported by the European Union (EU) 7th Framework Program MIRSURG (grant 224042), by the Ministry of Science and Innovation, Spain, through the Consolider Program SAUUL (grant CSD2007-00013), and by the European Office of Aerospace Research and Development (EOARD) through grant FA8655-09-1-3017.

References

1. G. Edwards, R. Logan, M. Copeland, L. Reinisch, J. Davidson, B. Johnson, R. Maciunas, M. Mendenhall, R. Ossoff, J. Tribble, J. Werkhaven, and D. O'Day, Nature **371**, 416 (1994).
2. J. Hildenbrand, J. Herbst, J. Wöllenstein, and A. Lambrecht, Proc. SPIE **7222**, 72220B (2009).
3. P. G. O'Shea and H. P. Freund, Science **292**, 1853 (2001).
4. M. Ebrahim-Zadeh and I. T. Sorokina, eds., *Mid-Infrared Coherent Sources and Applications*, 1st ed. (Springer, 2007).
5. K. T. Zawilski, P. G. Schunemann, T. M. Pollak, D. E. Zelmon, N. C. Fernelius, and F. K. Hopkins, J. Cryst. Growth **312**, 1127 (2010).
6. V. Petrov, P. G. Schunemann, K. T. Zawilski, and T. M. Pollak, Opt. Lett. **34**, 2399 (2009).
7. V. Petrov, G. Marchev, P. G. Schunemann, A. Tyazhev, K. T. Zawilski, and T. M. Pollak, Opt. Lett. **35**, 1230 (2010).
8. A. Peremans, D. Lis, F. Cecchet, P. G. Schunemann, K. T. Zawilski, and V. Petrov, Opt. Lett. **34**, 3053 (2009).
9. O. Chalus, P. G. Schunemann, K. T. Zawilski, J. Biegert, and M. Ebrahim-Zadeh, Opt. Lett. **35**, 4142 (2010).
10. M. Sheik-Bahae, D. C. Hutchings, D. J. Hagan, E. W. V. Stryland, IEEE J. Quantum Electron. **27**, 1296 (1991).